Digest Journal of Nanomaterials and Biostructures Vol. 20, No. 2, April - June 2025, p. 681 - 690

Bio fabrication techniques, optical characteristics and applications of TiO_2 in the environmental and medical sector

E. A. Razak, H. A. T. Al-Ogaili*
Department of Physics, College of Science, Wasit University, Kut, Iraq

Our study focuses on the bio-fabrication process and the environmental and medical applications of titanium dioxide (TiO2) nanoparticles synthesized in a green manner. Using plant extracts as eco-friendly agents, this research demonstrates how TiO2 nanoparticles of pure anatase phase can be formed with particle sizes ranging from 12.86 to 48.07nm. Synthesized nanoparticles have been examined for their structural, optical, and electronic properties using XRD, FE-SEM, UV-Vis spectroscopy, photoluminescence, Raman and FTIR spectroscopy. In this study, TiO_2 nanoparticles are investigated for their ability to break down organic dyes while simultaneously being investigated as glucose sensor elements. In experimental results, it has been demonstrated that methylene blue dye can be readily degraded by methyl orange dye, and that glucose can be reliably detected within a broad range (0.1-20mM) with sensitive biosensor mechanisms.

(Received March 20, 2025; Accepted June 20, 2025)

Keywords: TiO_2, PL, Biosensor, Electrochemical, Raman mode, Green route, Photocatalysis

1. Introduction

Over the last few years, nanomaterial studies have received an overwhelming amount of attention [1]. The field of nanotechnology deals with nanometer-sized materials in a variety of scientific fields, such as biotechnology, nanotechnology, physics, materials science, and chemistry, making it an empowering technology [2]. The application of Nanobiotechnology for preparing metallic nanoparticles is not only interesting, but it is also an important approach for creating hygienic, safe, and environmentally friendly events for the fusion and gathering of metallic nanoparticles [1]. Due to the growing need for ecologically friendly solvents and renewable materials, the biosynthesis of nanoparticles has received increasing attention over the past few years. Nanoparticles are useful in nontoxic chemicals, antibacterial, anticancer, antiviral, drug delivery, diagnostics and environmental amenable solvents [3]

There are several types of nanotechnology, including ones that have at least one dimension between 1-100 nanometers [4-5]. As a result of their antibacterial properties, resistance against microbes, drug delivery, antibiotics characteristics, and immune chromatography [6], metal oxide nanoparticles have received considerable attention in medical applications, TiO_2 is one of the most important for a variety of applications including self-cleaning and electrochemical sensors [7].

In addition to having exceptional photocatalytic properties, titanium dioxide nanoparticles are also valuable materials in various fields related to the environment, industry, and energy. The unique photocatalytic properties of TiO_2 nanoparticles are due to the fact that they are capable of absorbing and converting ultraviolet (UV) or visible light energy into chemical reactions, primarily by generating electron-hole pairs on their surfaces. It has a large forbidden band, so radiation above UV wavelengths (above 3.2 eV) can only stimulate photocatalytic activity [8]. Daily, large quantities of unconsumed dyes are used in several industries, including printing, textiles, plastic, and cosmetics, as waste released into the effluent stream after coloring and are released into the environment [9]. A photocatalytic method can be used to remove hazardous residues from the environment in an environmentally friendly mannered. The techniques for treating wastewater with

* Corresponding author: hananabd81@gmail.com
https://doi.org/10.15251/DJNB.2025.202.681

photocatalysis it is used for the overall mineralization of organics. When compared to bulk equivalents, nanoparticles possess various properties, such as a high surface area, a large dimension, as well as improved morphology. Since nanotechnology has been attracting a great deal of interest, it is worth developing rapid, simple, cost-effective, and environmentally friendly methods to synthesize nanoparticles [10]

A biosensor can be applied in a wide variety of fields, including biomedical research, forensic investigation, drug discovery, point-of-care diagnostics, environmental monitoring and food safety [11]. TiO2's crystallinity is a key factor that affects its performance in many applications. As a result of trapping electrons and holes in the anatase and rutile phases, it has been found that a combination of these phases is highly efficient in photocatalytic applications. For jasmine flower, titanium dioxide nanoparticles (TiO2 NPs) were successfully synthesized by using the green synthesis method [12]. In this work, focused on the biofabrication of TiO_2 NPS from Anethum graveolens extract and applications in the electrochemical sensor and photo-catalyst for two dyes in addition to the characteristics

2. Methodology

2.1. Preparation of the plant extract

In the beginning, fresh Anethum graveolens leaves were collected from the market. Then dust and dirt were removed from the leaves by washing them in deionized water. Next, the leaves were dried for a week at room temperature. After that, the dried leaves were ground into powder. To prepare the extract approximately 25g of powdered leaves was mixed with 500 mL of DW. the mixture was left at room temperature and away from light for one day. filter paper was used to filter the solution [13].

2.2. Preparation of pure titanium oxide (NPs)

40M (titanium tetra isopropoxide) was added with 40ml of plant extract (Anethum graveolens) placed on a magnetic stirrer at 37 C for an hour. , Then add 2ml ammonia (NH_3)to the mixture until it reaches (pH) to (pH8) and so the solutions change colour and become thick, added to it and place on a magnetic stirrer at 50 C for 3 hours leave it until it dissolves and the solution becomes yellow coloured The solution is washed with distilled water three times[14], then the mixture is dried for a week at room temperature subsequently crush it with a pestle and put it in the oven at (600°C) for 2 h. After taking it out of the oven, crush it with the pestle to get TiO_2.

3. Results and discussions

3.1. XRD and FE-SEM results

Fig 1 shows the diffraction peaks of $Ti0_2$ NPs synthesized via an eco-friendly green synthesis from Anethum graveolens extract obtained from XRD analysis corresponded crystallographic planes are (101) (004) (200) (211) (204) and (220) at angles 26 25.54° 37.99°, 48.15°, 53.99°, 63.00°, and 70.52 the diffracted pattern perfectly matched the anatase titanium dioxide phase described in JCPDS card 01-073-1764. A well-defined peak demonstrating high crystallinity and phase purity can be seen in the synthesized material, where Full Width at Half Maximum values are mentioned in Table 1. Also mentioned analysis of crystallite size was performed using the Debye-Scherrer equation, and the nanocrystalline of synthesized TiO_2 mean particle size is 25,940 nm By employing green chemistry, pure anatase TiO2 nanoparticles were produced exhibiting distinct crystallization features without peak additions in the X-ray diffraction pattern [15].

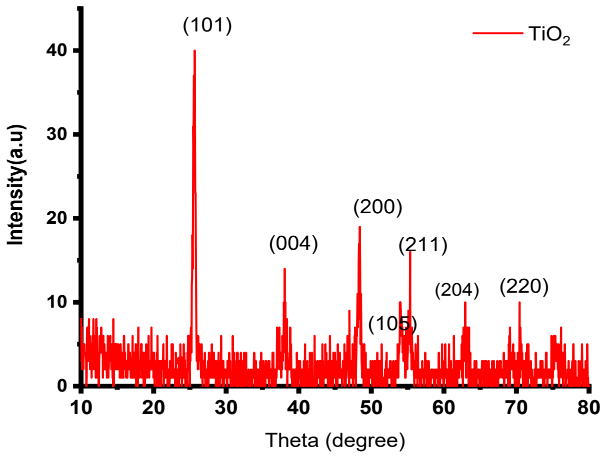

Fig. 1. XRD pattern of TiO_2.

Table 1. XRD parameters and crystallite size analysis.

2 theta (degree)	hkl	FWHM (deg)	2theta(rad)	FWHM(rad)	D(nm)	Matched by
25.54936	101	0.362112	0.223	0.006	22.487	01-073-1764
37.9902	004	0.271584	0.332	0.005	30.924	
48.35272	200	0.181056	0.422	0.003	48.077	
53.99137	105	0.271584	0.471	0.005	32.816	
55.33274	211	0.543168	0.483	0.009	16.508	
63.00223	204	0.724224	0.550	0.013	12.860	
70.52866	220	0.543168	0.615	0.009	17.906	
Mean particle size					25.940	

Anethum graveolens extract was utilized to synthesize TiO_2 nanoparticles (anatase phase) via an eco-friendly method. Figure (2) shows FE-SEM images of the result. It appears in the images that the nanoparticles in the sample are well-dispersed quasi-spherical particles, with uniform sizes. The 10,000x image shows the aggregates of nanoparticles with a cauliflower morphology, yet the 60,000x image reveals single nanoparticles of sizes between 28.46 nm to 46.58 nm with an average of 35.23 nm.

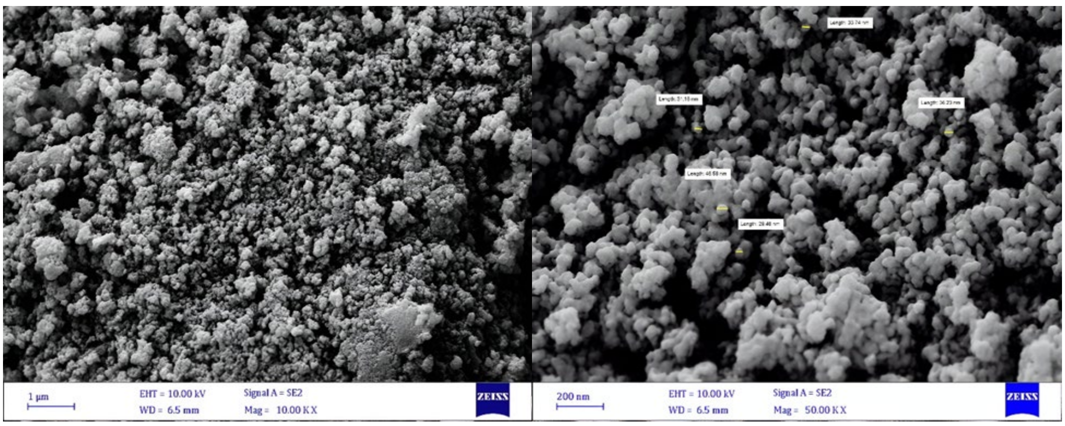

Fig. 2. FE-SEM images of TiO_2 nanoparticles synthesized by an eco-friendly method.

The agglomeration of nanoparticles occurs because of their high surface energy and because bioactive compounds from the plant extract function as stabilizing agents. The high surface energy of nanoparticles and the presence of bioactive compounds in plant extract stabilize nanoparticles, causing them to agglomerate. As a result of a green synthetic method [16, 17].

3.2. UV-visible

TiO_2NPs are important for their optical and electronic properties. Fig.3- graph(a) indicates TiO_2 absorbs UV light at 380 nm wavelength. With this strong absorption peak, the material is able to absorb ultraviolet light effectively, an important characteristic of photocatalytic purposes. TiO2 materials are usually characterized by a decrease in absorption toward longer wavelengths (visible light region). In **Fig. 3**- Graph (b), this feature is demonstrated through the analysis of Tauc plots to determine the bandgap energy value. According to laboratory measurements, the plotted data extend to a wavelength of approximately 299 eV, which represents TiO2's optical bandgap. Because TiO2 has a bandgap energy of 2.99 eV, it is primarily transparent in the visible range while absorbing UV light A combination of the bandgap properties of TiO2 and the optical absorption properties make it an ideal material for photocatalysis and optoelectronic devices [17].

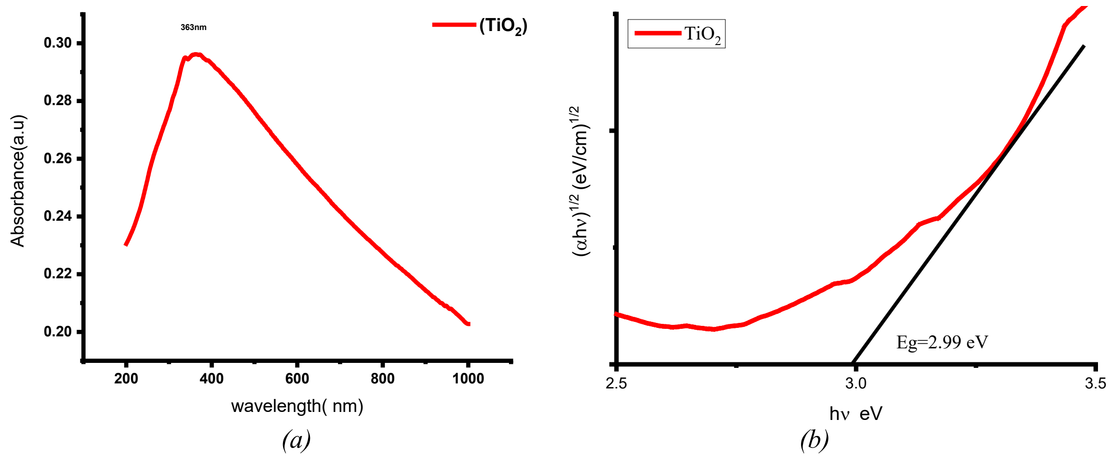

Fig. 3. (A) UV-Vis spectrum and (B) Tauc plot of TiO_2 optical bandgap.

3.3. Photoluminescence

In **Fig. 4**, A TiO_2 photoluminescence spectrum can be identified by identifying three main emission peaks that provide essential information about electronic structures and optical transitions. The first peak represents the direct energy of TiO_2 about 3.4 eV, at 512 nm (2.4 eV), emission intensity indicates a mid-gap state caused by crystallographic defects or oxygen defects within the crystal structure of TiO_2, which occurs due to crystallographic faults. It is believed that radiant recombination occurs strongly at (735) nm (1.6 eV) as a result of deep-level trap states that are generated by surface defects and intrinsic structural irregularities. This enables us to study the electronic states and charge movements throughout the materials by determining the intensity ratios of peaks in emission [18].

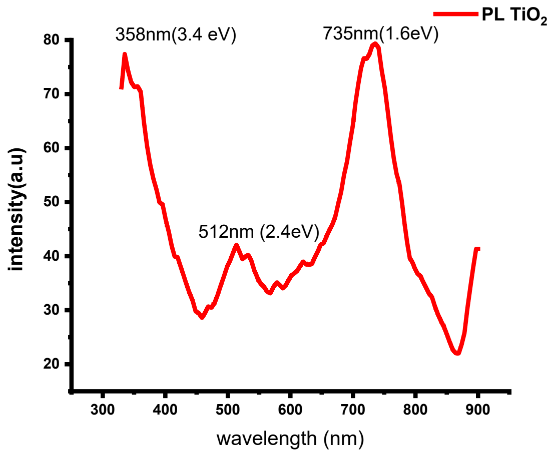

Fig. 1. Photoluminescence (PL) spectrum of TiO_2.

3.3. Raman modes and FTIR

Using Raman spectroscopy, Fig. 5 shows that there are many distinct peaks over a broad spectral range (0-4500 cm) that exhibit a rich vibrational signature. A peak at 788 cm^1 and 1152 cm^1 is the result of fundamental vibrations, whereas the distinctive peak at 227 cm^1 is the result of lattice vibrations.

Various intermediate vibrational modes can be observed in the Raman spectra, namely 1592 cm^{-1}, 1982 cm^{-1}, 2376 cm^{-1}, and then higher frequency peaks at 3322 cm^{-1}, 3723 $cm^{-1}$and 4066 cm^{-1} . A sharp well-resolved peak indicates structural order and crystallinity levels in the material, whereas peak intensity variations and locations reveal information about molecular symmetry and bond strength. The wide range of vibrational modes indicates that the material possesses complex structural elements with diverse chemical bonds and vibrational interactions [16,20,21].

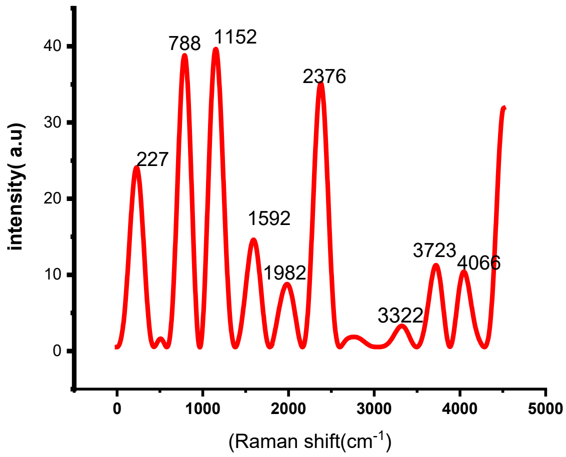

Fig. 2. Raman spectrum showing characteristic vibrational modes with major peaks.

There are several characteristic vibrational bands evident in the FTIR spectrum of TiO_2 NPs from Anethum graveolens extract that provide information about their molecular structure and chemical composition:

Fig. 6 illustrates that the broad absorption band at 3269 cm-1 is related to stretching vibrations of O-H groups, which indicates that the TiO_2 nanoparticles have water molecules and hydroxyl groups on their surfaces. The hydroxylation of the surface is common in metal oxide nanoparticles synthesized through green syntheses and plays an essential role in their photocatalytic properties.

During green synthesis, the TiO_2 surface shows a dominant absorption peak at 1637 cm1 which is associated with the bending vibrations of H-O-H molecules, confirming its association with water molecules and also suggesting successful surface modification.

There are two bands observed at 970 cm1 and 604 cm1 in the lower wavenumber region, representing stretching vibrations of Ti-O-Ti and bending vibrations of Ti-O2. These bands confirm that TiO2 crystal lattices are forming. According to the XRD results in the provided document, these peaks indicate that a successful synthesis of TiO2 nanoparticles in the anatase phase has been achieved.

It appears that these FTIR features are indicative of a successful synthesis of TiO_2 NPs with hydroxyl groups bound to the surface, which could contribute to their environmental applications, especially promoting photocatalytic degradation [20,24].

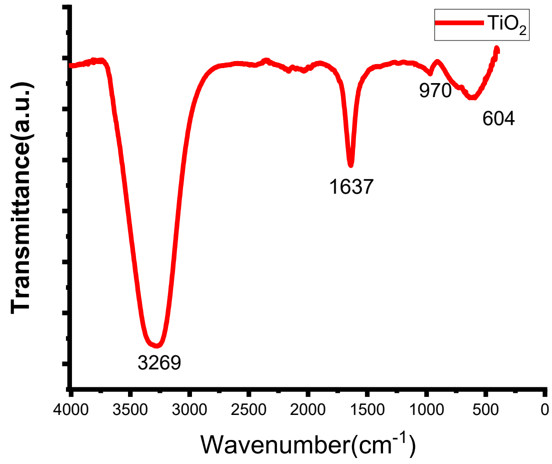

Fig. 6. FTIR Spectrum of TiO2.

3.4. Photocatalytic activity

The UV-Vis absorption spectra of Fig. 6 (A & B) display the photocatalytic destruction process of organic dyes through TiO_2 nanoparticles under different time conditions.

Fig. 6 (A) displays the absorption spectral data that demonstrates peak intensity decline from (0 to 125 minutes) for the TiO_2-MO (TiO_2-Methyl Orange) system as it degrades the organic dye progressively through photocatalysis. The first recorded spectrum from 0 minutes displays a standard peak at 480 nm that corresponds to the absorption spectrum of methyl orange dye. During the reaction period, the peak intensity decreases systematically which indicates that TiO2 nanoparticles display efficient dye molecule decomposing capability. The fundamental characteristics analyzed in the work including the 2.99 eV bandgap explain the degradation mechanism. The photocatalytic reaction begins after TiO_2 absorbs UV light that creates pairs between electrons and holes. A sequence of water and oxygen interactions with charge carriers from TiO2 produces reactive oxygen species leading to the deterioration of organic dye molecules. The absorption intensity decreases gradually while simultaneously the dye concentration decreases as the compounds transform into basic substances.

A different time scale (0-150 min) characterizes the degradation process of MB-TiO_2 (Methylene Blue-TiO_2) in **Fig.6 (B).** The main peak at 660 nm displayed a major reduction throughout the experiment until it faded completely in the 150-minute. The synthesized TiO_2 nanoparticles display effectiveness in eliminating various classes of organic dyes. The photocatalytic process operates efficiently due to the structure of the TiO_2 pure anatase phase with crystallite sizes between 12.86-48.07 nm which creates ideal conditions for photocatalytic surface reactions [22,23].

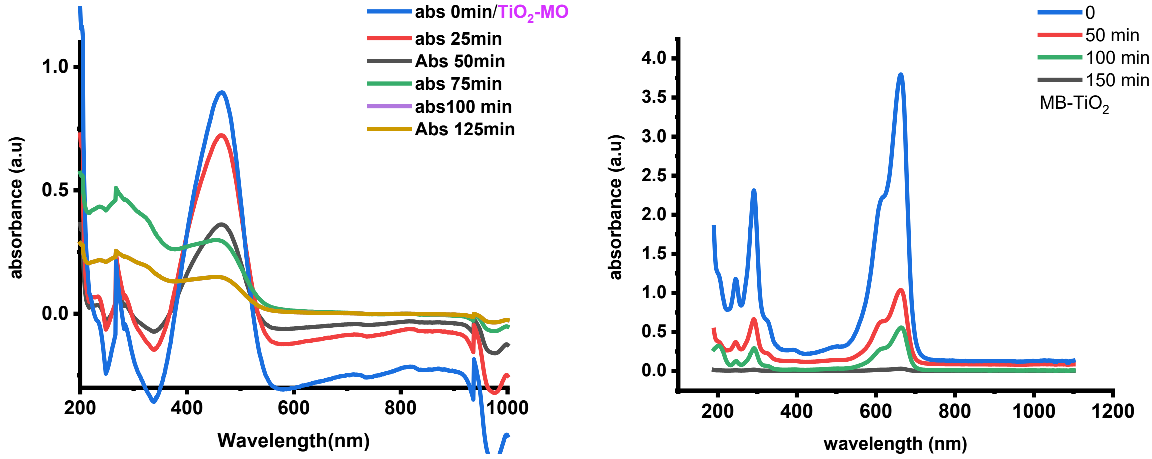

(a) *(b)*

Fig. 3. Photocatalytic process of organic dyes TiO2 nanoparticles under different time conditions (A) TiO_2-MO (TiO_2-Methyl Orange) (B) MB-TiO_2 (Methylene Blue-TiO_2).

3.5. Biosensor analysis results

Results from electrochemical examinations of the TiO2-based glucose sensing system prove excellent outcomes through multiple analytical tests. TiO2 electrode surface shows three distinct oxidation peaks during chronoamperometric analysis where the peak intensities decrease from 200 nA to 100 nA Figure 8. Analysis shows peaks that start with distinct quick elevation and finish with a gradual reduction of current until reaching a steady state which implies efficient signal restoration and proper charge transfer.

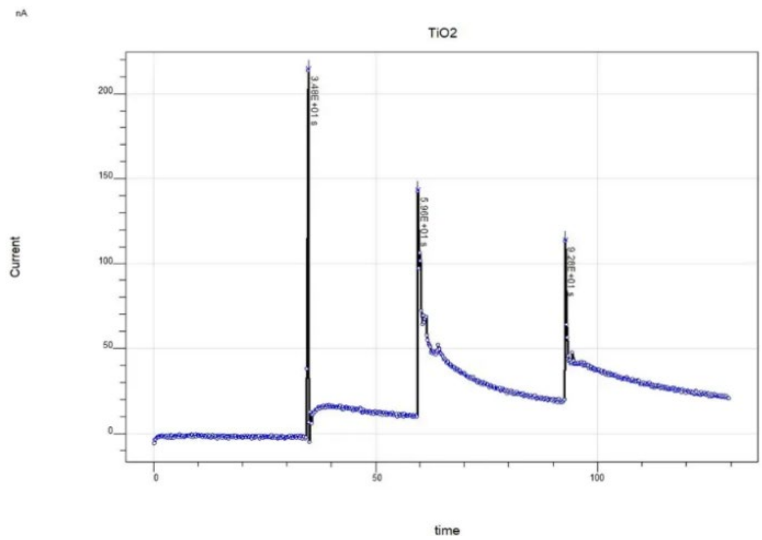

Fig. 4. Amperometric response of TiO_2 electrode showing three sequential current peaks over time.

The potential cycling measurements shown in **Fig.9** exhibit six cycles that maintain identical patterns throughout between the -2V and +2V range ensuring system stability and precision. Insights from potential cycling show that raising glucose concentration from zero leads to progressively extensive current signatures starting from 0.1mM (green) up to 10mM (red) and 20mM (blue). The evidence shows the sensor performs quantitative detection due to its response following concentration patterns.

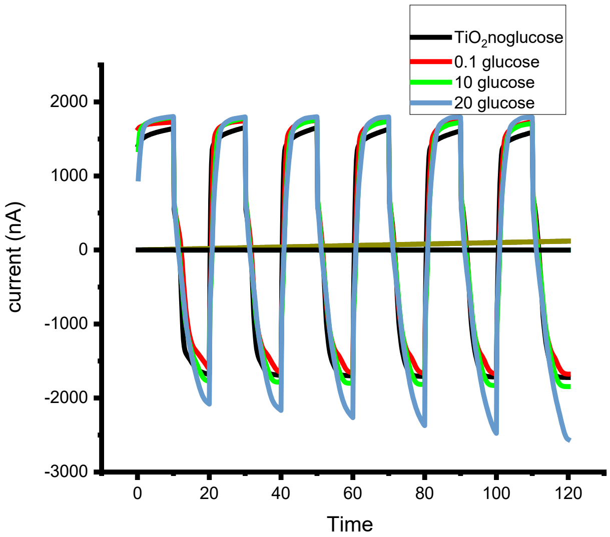

Fig. 5. Cyclic potential measurements of TiO2 electrode with varying glucose concentrations (0-20mM) showing six repeated cycles.

The cyclic voltammogram Figure 10 shows reaction kinetic processes in a potential range between -1.0V to +1.0V. A direct correlation exists between glucose concentration and the size of oxidation and reduction peaks which appear in the voltammetric profiles. Scan hysteresis along with systematic peak movement in cyclic voltammograms gives information about reaction reversibility and changes to reaction kinetics as concentration increases [24].

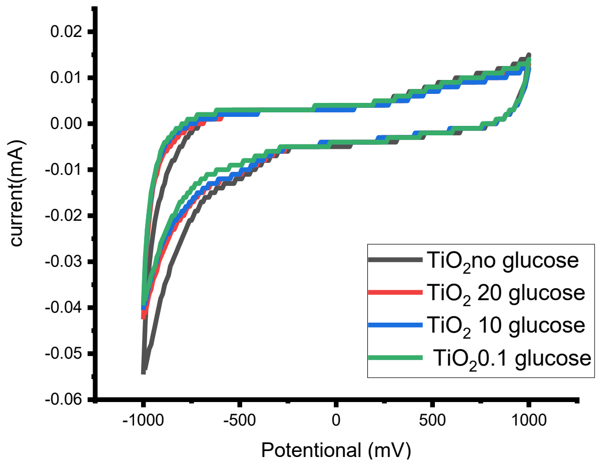

Fig. 6. Cyclic voltammograms of TiO2 in different glucose concentrations showing concentration-dependent current response.

Measurement results confirm the fundamental operational features of the TiO_2-based glucose sensor system. The system achieves high sensitivity based on its ability to produce differing current measurements for various glucose concentrations and its predictable repetitive results alongside its detection capacity spanning from 0.1mM to 20mM. A quick response time shown through high current peak intensity together with reliable baseline measurements and reversible electrochemical reactions demonstrates the strong detection capabilities of the sensor. The data indicates that TiO_2 functions well as an electrode material for glucose detection which could be applied in biosensing alongside environmental monitoring clinical diagnostics and food industry quality control systems. This electrochemical sensing platform achieves validity through the combined analytical data obtained from these three investigative methods which reveals complete reaction mechanism information and sensor behaviour at various concentration levels [25,26].

4. Conclusion

In research, green manufacturing methods have been shown to produce TiO2 nanoparticles with appropriate environmental properties. It is demonstrated that the produced TiO2 nanoparticles have a high crystalline structure, and uniform appearance, along with good optical properties with a bandgap measurement of 2.99 eV, as well as uniform optical behaviour.. In addition to photocatalysis testing, electrochemical research demonstrates that these materials could be used for glucose bio-sensing. This method provides complete information on the properties of the material using multiple techniques with performance data. A study suggests that eco-friendly TiO2 nanoparticles are capable of being used for water purification and biosensing systems through sustainable methods of protecting the environment. This glucose sensor system has a broad sensitivity range and steady performance characteristics, making it ideal for medical and environmental surveillance.

References

[1] S. Subhapriya, P. Gomathipriya, Microbial Pathogenesis,2018, 116, 215-220; https://doi.org/10.1016/j.micpath.2018.01.027

[2] N. Shahcheraghi, H. Golchin, Z. Sadri, Y. Tabari, F. Borhanifar, S. Makani, Biotechology, 2022, 12(3), 65; https://doi.org/10.1007/s13205-021-03108-9

[3] G. Karunakaran, K. G. Sudha, S. Ali, E. B. Cho, Molecules, vol. 28, no. 11, Jun 2 2023; https://doi.org/10.3390/molecules28114527

[4] D. D. Ganji, S. H. H. Kachapi, Application of Nonlinear Systems in Nanomechanics and Nanofluids Eds. Oxford: William Andrew Publishing, 2015, pp. 1-11; https://doi.org/10.1016/B978-0-323-35237-6.00001-7

[5] G. Nabi, W. Raza, M. Tahir, Journal of Inorganic and Organometallic Polymers and Materials, vol. 30, no. 4, pp. 1425-1429, 2020; https://doi.org/10.1007/s10904-019-01248-3

[6] L. Wang, C. Hu, L. Shao, Int J Nanomedicine, vol. 12, pp. 1227-1249, 2017; https://doi.org/10.2147/IJN.S121956

[7] J. Jenima et al., Heliyon, vol. 10, no. 20, p. e39238, 2024/10/30/ 2024; https://doi.org/10.1016/j.heliyon.2024.e39238

[8] M. A. Barakat, R. Kumar, Photocatalytic Activity Enhancement of Titanium Dioxide Nanoparticles: Degradation of Pollutants in Wastewater, 2015; https://doi.org/10.1007/978-3-319-24271-2_1

[9] J. Zhang et al., Separation and Purification Technology, vol. 329, p. 125225, 2024/01/15/ 2024; https://doi.org/10.1016/j.seppur.2023.125225

[10] A. Haleem, M. Javaid, R. P. Singh, R. Suman, S. Rab, Sensors International, vol. 2, p. 100100, 2021/01/01/ 2021; https://doi.org/10.1016/j.sintl.2021.100100

[11] G. Li et al., Dalton Transactions, no. 45, pp. 10078-10085, 2009; https://doi.org/10.1039/b908686b

[12] M. Aravind, M. Amalanathan, M. S. M. Mary, SN Applied Sciences, vol. 3, pp. 1-10, 2021; https://doi.org/10.1007/s42452-021-04281-5

[13] Abed FG, Jubeir NJ, Al Ogaili, HAT. AIP Conference Proceedings., 2024, 2922(1), 040006; https://doi.org/10.1063/5.0183132

[14] Saad Khalid Rahi, RusulAdnan Al-Wardy, Hanan Abd Ali Thjeel Al Ogaili, Baghdad Science Journal. 2025, Vol.22,no.4,p.1250-1259.https://doi.org/10.21123/bsj.2024.8208

[15] S. V. S. Mudrakola et al., Green Processing and Synthesis, vol. 13, no. 1, p. 20230182, 2024; https://doi.org/10.1515/gps-2023-0182

[16] S. Challagulla, K. Tarafder, R. Ganesan, S. Roy, Scientific reports, vol. 7, no. 1, p. 8783, 2017; https://doi.org/10.1038/s41598-017-08599-2
[17] M. Huston, M. DeBella, M. DiBella, A. Gupta, Nanomaterials, vol. 11, no. 8, p. 2130, 2021; https://doi.org/10.3390/nano11082130
[18] Y.-J. Chen, T.-S. Lin, Applied Sciences, vol. 10, no. 18, p. 6353, 2020; https://doi.org/10.3390/app10186353
[19] K. Piler, C. Bahrim, S. Twagirayezu, T. J. Benson, Advances in Catalysis, vol. 66: Elsevier, 2020, pp. 109-233; https://doi.org/10.1016/bs.acat.2020.09.001
[20] A. León et al., Applied Sciences, vol. 7, no. 1, p. 49, 2017; https://doi.org/10.3390/app7010049
[21] H.A.T. Al-Ogaili, R.A Al-Wardy, Journal of Physics: Conference Series .2020, 1591, 012008; https://doi.org/10.1088/1742-6596/1591/1/012008
[22] H.A.T.Al-Ogaili , , N.J. Jubier, , A.A Thamer .Digit J. Nanomaterials. Biostructure. 2025 January ;20(1): 365–372 .https://doi.org/10.15251/DJNB.2025.201.365
[23] J. J. Murcia Mesa et al., Ciencia en Desarrollo, vol. 8, no. 1, pp. 109-117, 2017; https://doi.org/10.19053/01217488.v8.n1.2017.5352
[24] M. Söyleyici Cergel, E. Demir, F. Atay, Ionics, vol. 25, pp. 4481-4492, 2019; https://doi.org/10.1007/s11581-019-02986-7
[25] M. Christwardana, Y. Chung, Y. Kwon, NPG Asia Materials, vol. 9, no. 6, pp. e386-e386, 2017; https://doi.org/10.1038/am.2017.75
[26] S. Saha et al., Scientific Reports, vol. 7, no. 1, p. 6855, 2017; https://doi.org/10.1038/s41598-017-06926-1